molecular pharmaceutics

Article

pubs.acs.org/molecularpharmaceutics

Drug Distribution to Retinal Pigment Epithelium: Studies on Melanin Binding, Cellular Kinetics, and Single Photon Emission Computed Tomography/Computed Tomography Imaging

Anna-Kaisa Rimpelä,[*,†] Mechthild Schmitt,[†] Satu Latonen,[†] Marja Hagström,[†] Maxim Antopolsky,[†] José A. Manzanares,[§] Heidi Kidron,[†] and Arto Urtti[†,‡]

[†]Centre for Drug Research, Division of Pharmaceutical Biosciences, Faculty of Pharmacy, University of Helsinki, P.O. Box 56, FI-00014 Helsinki, Finland

[‡]School of Pharmacy, University of Eastern Finland, P.O. Box 1627, FI-70211 Kuopio, Finland

[§]Department of Thermodynamics, Faculty of Physics, University of Valencia, E-46100 Burjassot, Spain

Supporting Information

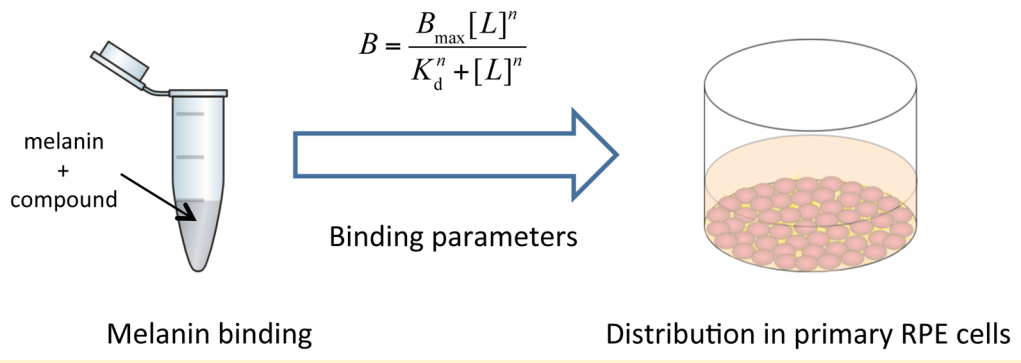

ABSTRACT: Melanin binding is known to affect the distribution and elimination of ocular drugs. The purpose of this study was to evaluate if the extent of drug uptake to primary retinal pigment epithelial (RPE) cells could be estimated based on *in vitro* binding studies with isolated melanin and evaluate the suitability of single photon emission computed tomography/computed tomography (SPECT/CT) in studying pigment binding *in vivo* with pigmented and albino rats. Binding of five compounds, basic molecules timolol, chloroquine, and nadolol and acidic molecules methotrexate and 5(6)-carboxy-2′,7′-dichlorofluorescein (CDCF), was studied using isolated melanin from porcine choroid-RPE at pH 5.0 and 7.4. The uptake to primary porcine RPE cells was studied with timolol, chloroquine, methotrexate, and CDCF. The cell study setting was modeled using parameters from the *in vitro* binding study. *In vivo* kinetics of 3-[I-123]-iodochloroquine was studied by the SPECT/CT method in albino and pigmented rats. All basic compounds bound to melanin at both pH values, whereas the acidic compounds bound more at pH 5.0 than at pH 7.4. The basic compounds (chloroquine, timolol) showed significant cellular uptake, unlike the acidic compounds (methotrexate, CDCF). On the basis of the modeling, melanin binding was a major factor governing the overall drug distribution to the RPE cells. Likewise, melanin binding explained distribution of 3-[I-123]-iodochloroquine in the pigmented RPE, whereas drug accumulation was not seen in the albino rat. This study demonstrates the suitability of noninvasive SPECT/CT imaging in monitoring ocular melanin binding *in vivo*. These studies are a useful step toward understanding the pharmacokinetic impact of melanin binding.

KEYWORDS: *ocular pharmacokinetics, melanin binding, retinal pigment epithelium, binding parameters, SPECT/CT*

INTRODUCTION

Ocular melanin binding of drugs has been studied since Potts introduced the first *in vitro* binding studies with isolated uveal melanin in 1964.[1] The effect of melanin binding on the kinetics of ocular drug delivery still remains, however, inadequately understood. Melanin is found in many tissues including the eye, skin, hair, brain, and inner ear. In the eye, melanin is found in the uvea (iris, ciliary body, choroid) and the retinal pigment epithelium (RPE). Because of its wide expression, melanin may affect the kinetics of drugs administered through several routes: topically administered eye drops, periocular and intravitreal injections, and systemically administered drugs. The ocular drug, betaxolol, has been found at 100-fold higher concentrations in

Special Issue: Ocular Therapeutics: Drug Delivery and Pharmacology

Received: October 16, 2015
Revised: December 23, 2015
Accepted: January 7, 2016
Published: January 7, 2016

DOI: 10.1021/acs.molpharmaceut.5b00787
Mol. Pharmaceutics 2016, 13, 2977−2986

ocular pigmented tissues compared to nonpigmented tissues during chronic dosing as eye drops.[2] Another ocular drug, atropine, has a weaker but considerably longer effect in pigmented than in nonpigmented eyes due to melanin binding.[3] Additionally, the systemically given antipsychotic, chlorpromazine, is known to accumulate in the uvea due to melanin binding, and this may lead to retinal toxicity.[4] Thus, understanding melanin binding is important for ocular as well as systemic drug therapy.

Melanin is a polyanionic polymer located in cell organelles called melanosomes, within pigmented cells. In the melanosomes, melanin is bound to a protein matrix, that is, however, thought to have little effect on the binding of drugs.[5] The pH inside melanosomes is considered to be acidic.[6,7] The binding thus takes place in an acidic environment, which is generally not the case in *in vitro* binding studies.[8−10] Furthermore, the effects of other cellular factors, such as the lipid membrane of melanosomes, membrane transporters, and drug access into the pigmented cells, have not been evaluated together with melanin binding. To better understand and predict the effect of melanin binding on ocular pharmacokinetics of drugs, these factors need to be taken into account.

The parameters for melanin binding, maximum binding capacity (B_{max}), and dissociation constant (K_d) have generally been calculated from the Langmuir isotherm.[8−10] Both one- and two-site binding models have been used. The Langmuir isotherm assumes that drug binding to melanin occurs on localized sites. Many drugs are, however, large compared to the distance of binding moieties (functional groups) on melanin and can bind simultaneously to many of them.[11] This hampers the suitability of different isotherms to depict drug−melanin binding. There is a large disparity of binding parameter values in literature because the values are dependent on the drug concentrations that were used in the assays.[11] Therefore, drawing conclusions from these values can be difficult, and the physical meaning of the numbers is often obscure. A robust and physically relevant method for binding analyses is needed.

Predicting *in vivo* effects of melanin binding based on *in vitro* results is challenging, and the effect of melanin binding on pharmacokinetics and pharmacodynamics is not well understood. In this study, we aimed to generate new methods for improved pharmacokinetic understanding of melanin binding of drugs. More specifically, ocular melanin binding of five compounds was evaluated and binding parameters calculated with a new robust and physically relevant approach.[11] Cellular uptake of the drugs was experimentally studied with pigmented primary RPE cells, and the uptake was estimated based on melanin binding parameters. Finally, we introduce noninvasive single photon emission computed tomography/computed tomography (SPECT/CT) imaging for melanin binding studies *in vivo*. These studies will be a useful step toward reliable prediction and understanding of pharmacokinetic impact of melanin binding.

EXPERIMENTAL SECTION

Materials. Chloroquine diphosphate salt, nadolol, 5(6)-carboxy-2′,7′-dichlorofluorescein (CDCF), methotrexate, and dimethyl sulfoxide (DMSO) were purchased from Sigma-Aldrich (St. Louis, MO, USA) and timolol maleate salt from MP Biomedicals (Santa Ana, CA, USA). DMSO was used as a solvent for the highest concentrations of stock solutions, which were then diluted with phosphate buffered saline (PBS) (pH 7.4, without $CaCl_2$ and $MgCl_2$, 1.06 mM KH_2PO_4, 155 mM NaCl, 2.97 mM Na_2HPO_4) (Gibco, Invitrogen, NY, USA) or citrate buffer (pH 5, 20.5 mM $C_6H_8O_7$, 29.5 mM $C_6H_5O_7Na_3$).

Cells were cultured in Dulbecco's modified Eagle medium (DMEM) 31885 (Gibco) supplemented with 10% fetal bovine serum (FBS), 100 U/mL of penicillin, and 100 μg/mL of streptomycin. Cells were detached with 0.25% trypsin-EDTA (Gibco) and washed with DPBS (Gibco, with or without $CaCl_2$ and $MgCl_2$).

All chemicals used in radiolabeling were purchased from Sigma-Aldrich. $Na^{123}I$ was purchased from MAP Medical Technologies Oy (Finland), and all buffers for labeling were prepared *in situ*.

Isolation of Melanin Granules. The melanin used in the binding studies was isolated from the RPE and choroid of porcine eyes. The method used was modified from earlier studies.[8,10] Fresh porcine eyes were obtained from a slaughter house (HK Ruokatalo, Forssa, Finland) and kept on ice during the transport. Extraocular material was cleaned from the eyes with scissors, and the eyes were dipped in ethanol and then in PBS before cutting. The eyes were cut circumferentially behind the limbus, and the anterior part of the eye with the vitreous was gently removed. The remaining eye cup was turned inside out. The neural retina was gently removed uncovering the RPE and the choroid. The RPE-choroid was separated from the sclera, placed in PBS (pH 7.4), and stored at −20 °C until melanin isolation. Subtilisin protease type VIII from *Bacillus licheniformis* (Sigma-Aldrich) was added to the RPE-choroid in PBS, the amount of the protease being at least 30 mg/25 eyes. The suspension was incubated at 56 °C for 1 h with manual stirring every 10 min and then heated to 95 °C for 15 min to inactivate the protease. The suspension was centrifuged at 37 000*g* for 15 min, and the supernatant was discarded. The pellet was washed with PBS and centrifuged as above. The suspension was vacuum filtered on a Büchner funnel through filter paper. The filtrate was centrifuged at 37 000*g* for 15 min, and the precipitate was mixed with Milli-Q water and lyophilized overnight.

Zeta Potential of Melanin Granules. Zeta potential of the melanin granules was measured with Zetasizer Nano ZS (Malvern Instruments, Worcestershire, UK) at pH 5.0 (in citrate buffer) and pH 7.4 (in PBS), in the same buffers that were used in binding studies. Melanin suspensions of 1 mg/mL were made in both buffers. The suspensions were warmed to 37 °C, sonicated for 15 min, and diluted to a 0.2 mg/mL concentration for the measurement.

Binding Studies with Isolated Melanin. Melanin binding experiments were performed with five compounds: nadolol, timolol, chloroquine, CDCF, and methotrexate, at pH 5.0 and 7.4 in the concentration range of 0.25−250 μM, except the experiments with nadolol at pH 7.4 were done using concentrations of 0.5−500 μM, chloroquine at pH 5.0 with concentrations of 0.25−100 μM, and methotrexate was studied at pH 5.0 using 0.25−500 μM of the drug. Melanin suspension and test compound solutions were prepared just before every experiment. Melanin was mixed with PBS or citrate buffer to form a 2 mg/mL suspension. The suspension was sonicated for 15 min before incubation with the test compounds (70 μL of melanin suspension + 70 μL of compound solution) at 37 °C in a shaker (220 rpm). Three replicates were made of each experiment. After incubation, the melanin suspension was centrifuged at 21 000*g* for 15 min and the supernatant collected for analysis.

Calculation of Binding Parameters. *In vitro* melanin binding data were analyzed by using the Sips isotherm:

DOI: 10.1021/acs.molpharmaceut.5b00787
Mol. Pharmaceutics 2016, 13, 2977−2986

$$B = \frac{B_{max}[L]^n}{K_d{}^n + [L]^n} \quad (1)$$

as described by Manzanares et al.[11] For comparison, results were calculated by the generally used Langmuir binding isotherm for one (eq 2) and two (eq 3) classes of independent binding sites:

$$B = \frac{B_{max}[L]}{K_d + [L]} \quad (2)$$

$$B = \frac{B_{max1}[L]}{K_{d1} + [L]} + \frac{B_{max2}[L]}{K_{d2} + [L]} \quad (3)$$

where index 1 denotes the high-affinity sites, $K_{d1} < K_{d2}$. The maximum value of B is $B_{max1} + B_{max2}$ and corresponds to $[L] \gg K_{d2}$. Although the measures of the goodness of fit, such as the coefficient of determination, are generally good when using eq 3, the direct plot of B versus $[L]$ seldom evidences confidently the existence of two types of sites, and the interpretation of the values obtained for the parameters B_{max1}, B_{max2}, K_{d1}, and K_{d2} is often unclear.[11] The rationale and advantages of the use of the Sips isotherm have been reported in ref 11.

The Sips isotherm can also be conveniently presented as

$$\frac{1}{B} = \frac{1}{B_{max}} + \frac{1}{k[L]^n} \quad (4)$$

where $k \equiv B_{max1}/K_{d1}{}^n$. Thus, in a Scatchard plot, the binding curve is concave upward and diverges as $B \to 0$, and eq 4 can then be approximated as $B/[L] \approx k^{1/n}B^{(n-1)/n}$. The shape of the binding curve is very similar to that obtained when the isotherm corresponding to two classes of sites is represented in a Scatchard plot. The latter also yields a concave upward curve with linear asymptotes in the limits $B \to 0$ and $B \to B_{max1} + B_{max2}$. The maximum value of $B/[L]$ is $k \equiv B_{max1}/K_{d1} + B_{max2}/K_{d2}$ and corresponds to the limit $B = 0$.

Isolation of RPE Cells from Porcine Eyes. The RPE cells used for the cell uptake study were isolated from porcine eyes. The eyes were delivered and cleaned as described for melanin isolation. Twenty eyes were used to fill one T25 cell culture flask (Sarstedt, Nümbrecht, Germany) with RPE cells. The anterior part of the eye with the vitreous was removed in the same manner as in the isolation of melanin. The eye cup was then filled with PBS (without $CaCl_2$ and $MgCl_2$), which was removed after 10 min. The neural retina was carefully removed with tweezers. The eye cups were filled with 0.25% trypsin-EDTA and incubated for 30 min at 37 °C in a humidified atmosphere with 5% CO_2. The detached cells in the trypsin-EDTA solution were collected into 50 mL centrifuge tubes, and twice the volume of the trypsin-EDTA-cell solution of growth medium (10% (v/v) fetal bovine serum, 100 U/mL of penicillin, 100 μg/mL of streptomycin in DMEM 31885) was added. The tubes were centrifuged three times; first at 450*g* for 5 min, then twice at 200*g* for 2 min, in between replacing the supernatant with growth medium. The cells were suspended again in medium and transferred to the cell culture flask.

Cell Culture. Medium for the primary RPE cells in the cell culture flask was changed twice per week. The cells were seeded on a 48-well plate (Nunclon Delta surface, 1.1 cm^2/well, Thermo Scientific, Waltham, MA, USA) after 1−2 weeks in the cell culture flask. The cell monolayer was washed with prewarmed DPBS (without $CaCl_2$ and $MgCl_2$). The cells were incubated at 37 °C (5% CO_2) with 0.25% trypsin-EDTA for 5 min and then suspended in growth medium. Cell density was adjusted to 300 000 cells/mL. Two-hundred-fifty microliters (68.2×10^3 cells/cm^2) of cell suspension was added to each well and incubated overnight before the experiments. Cells in the cell culture flask were observed regularly with a light microscope (Leica, Wetzlar, Germany) to ensure the cells were dividing and contained melanin.

Cell Studies. Compound solutions were prepared aseptically from filter sterilized (Corning (MA, USA) syringe sterile filter with regenerated cellulose membrane, pore size 0.20 μm) stock solutions. Final compound solutions were diluted from the stock solutions with DMEM 31885. The concentration of DMSO in the final solutions did not exceed 1%.

Uptake experiments were performed with chloroquine (concentrations 0.29−4.1 μM), timolol (0.65−6.2 μM), methotrexate (1.1−12 μM), and CDCF (1.2−12 μM) with an incubation time of 20 h. The number of replicates was three (timolol, chloroquine) or two (methotrexate, CDCF). The cells were incubated at 37 °C (5% CO_2) with shaking (150 rpm).

Elimination studies were performed with chloroquine and timolol. Initially, the cells were incubated with the compound solutions for 20 h to reach equilibrium. The medium was changed to a blank medium, briefly washing the well with DBPS (with $CaCl_2$ and $MgCl_2$) in between, and thereafter, the increasing drug concentrations in the medium were analyzed at 0.5, 1, 2, 4, 6, 24, and 48 h.

Sample Analysis. Samples with expected concentrations over 0.1 μM were analyzed with UPLC (Acquity UPLC, Waters, Milford, MA, USA) with UV detection (Photodiode Array Detector, Waters, USA). The separation was carried out on a UPLC HSS T3 (1.8 μm, 2.1 × 50 mm^2) column (Waters) at 30 °C. Injection volume was 10 μL. Gradient mode was used for all the compounds with acetonitrile/15 mM phosphate buffer (pH 2) mobile phase. Gradient duration was 3−5 min depending on the sample.

For the samples with expected concentrations less than 0.1 μM, a mass spectrometric analysis with UPLC separation was used. The liquid chromatography instrument was Waters Acquity UPLC. The separation was carried out on a Waters UPLC HSS T3 (1.8 μm, 2.1 × 100 mm) column at 26 °C with an injection volume of 0.5 μL (0.1 μL for chloroquine). Gradient mode was used with acetonitrile (0.1% formic acid)/water (0.1% formic acid) mobile phase. Mass spectrometric measurements were carried out using Waters Xevo TQ-S triple quadrupole mass spectrometer with electrospray ionization with negative mode for CDCF and positive mode for the other compounds. Propranolol was used as an internal standard.

For the binding study with CDCF, fluorescence analysis was performed on a VarioskanFlash (Thermo Scientific, Waltham, MA, USA) fluorescence plate reader with 510 nm excitation and 535 nm emission. Samples were diluted 1:10 with 0.1 M sodium hydroxide before analysis.

Samples were also prepared of melanin incubated with PBS (without any test compounds) and treated as test samples to evaluate the effect of melanin on the analyses.

Modeling. Cell uptake was modeled with the compound concentrations used in the cell studies (5−300 μg of melanin/well; 75 000 cells in a well volume V_w = 250 μL). The values for maximum binding capacity B_{max} and equilibrium dissociation constant K_d were obtained from the binding study using the Sips isotherm. The initial concentration of the ligand outside the cells is $[L]_0$ (nmol/mL), and the final concentration of free ligand is $[L]$, both inside and outside the cells after equilibrium across the cell membrane is achieved. The fraction of ligand outside the cells

DOI: 10.1021/acs.molpharmaceut.5b00787
Mol. Pharmaceutics 2016, 13, 2977−2986

is $[L]/[L]_0$ and, hence, the fraction inside the cells is $f = 1 - [L]/[L]_0$. That is, from the total initial amount of ligand $[L]_0V_w$, the amount of ligand outside the cells is $[L]V_w$, and the amount of ligand (both free and bound to melanin) inside the cells is $[L]_0V_w - [L]V_w$. If we consider that the volume of the cells is $V_{cell} = 1\ \mu L$, the amount of free ligand inside the cells is $[L]V_{cell}$, and the amount of bound ligand inside the cells is $[L]_0V_w - [L](V_w + V_{cell})$. The amount of bound ligand inside the cells can also be evaluated as mB where B (nmol/mg) is the amount of bound ligand per melanin mass, and m (mg) is the melanin mass in the well. From eq 1, B can be evaluated as a function of the free ligand concentration $[L]$ and the parameters of the Sips isotherm. Thus, the melanin mass in the well can be formally evaluated as a function of the equilibrium free ligand concentration:

$$m = \frac{[L]_0V_w - [L](V_w + V_{cell})}{B} = \left(1 + \frac{K_d{}^n}{[L]^n}\right)\frac{[L]_0V_w - [L](V_w + V_{cell})}{B_{max}} \quad (5)$$

Since the free ligand concentration is $[L] = [L]_0(1 - f)$, where f is the fraction inside the cells, we can calculate m as a function of f for some values of the initial concentration $[L]_0$ and present its graphical representation exchanging the axis (i.e., f as a function of m), which is more natural from the experimental point of view.

Radiolabeling of Chloroquine with ^{123}I. Chloroquine was labeled with ^{123}I in the following manner to image its accumulation in pigmented tissues. To 0.2 mL of 0.5 M sodium dihydrophosphate buffer (pH 6.0), 0.1 mL of chloroquine diphosphate solution (153 mg/mL) was added. Then 0.02 mL of KI solution (1.25 mg/mL) and 0.8 mL of Na^{123}I solution (420 MBq) were added to the reaction mixture. The reaction was started by the addition of 0.02 mL of chloramine T solution (10 mg/mL).

After 15 min of incubation at room temperature, the reaction was stopped by the addition of 50 μL of 10% sodium thiosulfate solution. The reaction mixture was passed through an anion exchange cartridge (Discovery DSC-SAX 1 mL, Supelco Analytical, Pennsylvania, USA) to remove unreacted $^{123}I^-$. The eluted solution was purified on reversed phase (RP) C18 cartridges (Waters, USA). Final eluent was 70% acetonitrile. Addition of 0.05 mL of 0.1 M HCl to the eluent significantly improved recovery of the radiolabeled compound from the cartridge.

The reaction was performed in two equal portions to avoid dilution of PBS. The description above corresponds to a single portion. Finally, the product was concentrated in vacuum and dissolved in 2 mL of sterile saline solution and taken for animal experiments.

***In Vivo* Imaging.** This study was approved by the Finnish National Animal Experiment Board (permission number: ESAVI/3631/04.10.03/2012) and performed in accordance with Good Laboratory Practices for Animal Research. The 12–14 weeks old pigmented inbred Dark Agouti rats (DA/OlaHsd, Harlan Laboratories, The Netherlands) and albino inbred Fischer 344 rats (F344/NCrHsd, Harlan Laboratories, U.K.) were quarantined for 1–3 weeks before the start of the experiment. Rats were housed at 22 °C under a 12 h light–dark cycle. Commercial food pellets (Teklad Global 16% Protein Rodent Diet, Harlan Laboratories Inc., USA) and tap water were freely available before and during the study. On the study day, DA rats weighed 236–281 g and F344 rats 285–295 g.

To reduce ^{123}I labeled drug accumulation into thyroid, 9.1–12.9 mg/kg of 25.6–30.4 mg/mL iodine (potassium iodide powder (Sigma-Aldrich, St. Louis, MO, USA) in sterile saline (Sigma-Aldrich Company, U.K.)) was given via intragastric injection to the rats 1 h prior to drug administration. Rats were maintained under inhalation anesthesia with isoflurane (Attane vet 1000 mg/g Isofurain, Piramal Healthcare U.K. Limited, U.K.; Vetflurane 1000 mg/g, Virbac AnimalHealth, Carros, France) in oxygen gas during drug administration and imaging. Anesthesia induction was done with 4.5% isoflurane and maintained with 2–3% isoflurane. A heated bed in SPECT/CT machinery maintained body temperature of the animals. ^{123}I-labeled drugs were administered intravenously to the tail vein with a catheter needle (26 gauge, BD Neoflon, Singapore).

SPECT imaging was performed using a preclinical four-headed gamma ray camera with 1.0 mm multipinhole collimators (NanoSPECT/CT, Bioscan Inc., USA). Anatomical CT images were acquired with 45 kVp tube voltage X-ray camera in 180 projections. Studies with ^{123}I-chloroquine were conducted with two DA rats and one F344 rat. The rats received 49–57 MBq of ^{123}I-chloroquine intravenously in doses of 100–200 μL. Doses were obtained with a dose calibrator (Capintec Inc. CRC-25R, New Jersey, USA).

SPECT images were acquired from postinjection time points 0 h with 3 × 15 min interval (dynamic scan), 4 h, 8 h, and 24 h with 30–48 min interval (static scan). Longer intervals for 24 h time points were used to get better quality in the pictures. SPECT scanning was conducted with 24 projections using time per projection of 18, 20, 40, 50, and 60 s for whole body, and 150 and 300 s for head scans.

The SPECT images were reconstructed with HiSPECT NG software (Scivis GmbH, Germany) and CT images with CTReco (Bioscan Inc., USA). After reconstruction, images were fused and analyzed with VivoQuant (Bioscan Inc., USA). Volumes of interest (VOIs) were drawn manually to the areas of assumed melanin binding. Activity within each VOI was recorded, corrected for radioactive decay, and normalized to the activity at the time of injection.

Statistics. Results are presented as the mean ± standard error of mean, unless otherwise stated. The statistical significance of the difference in zeta potential of melanin granules in the two buffers were analyzed by Students t test using SigmaPlot software (Systat Software Inc., San Jose, CA, USA).

RESULTS

Binding Studies with Isolated Melanin. Zeta potential of the melanin granules was measured in PBS (pH 7.4) and citrate buffer (pH 5.0). The resulting values were −20.3 ± 0.3 mV and −17.1 ± 1.1 mV for the PBS and citrate buffer, respectively. There was a significant difference between the zeta potentials in the two buffers ($p = 0.048$).

All the basic compounds, timolol, nadolol, and chloroquine, bound to melanin at pH 7.4 and 5.0 (Figure 1). The binding of these compounds was not significantly affected by the pH. Chloroquine binding was most extensive (92–99.6% at pH 7.4, 75–99.5% at pH 5.0), while timolol binding was 11–21% at pH 7.4 and 18–33 at pH 5.0 and nadolol binding 8–24% at pH 7.4 and 17–27% at pH 5.0.

The acidic compounds, methotrexate and CDCF, showed low binding levels at pH 7.4 (less than 8%), but their binding was much higher at pH 5.0 (Figure 1).

Binding parameters were analyzed based on the Sips isotherm and Langmuir binding isotherms for two classes of independent

DOI: 10.1021/acs.molpharmaceut.5b00787
Mol. Pharmaceutics 2016, 13, 2977–2986

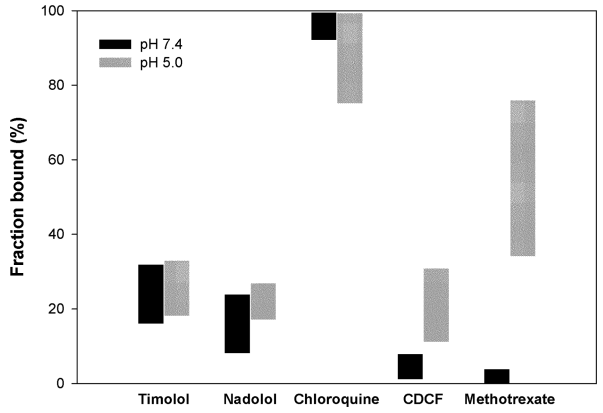

Figure 1. Range of binding of timolol, nadolol, chloroquine, methotrexate, and CDCF to isolated porcine choroid-RPE melanin at pH 5.0 and 7.4 with starting concentrations of 0.25−100 μM (nadolol pH 7.4 0.5−100 μM). Binding percentage was the highest with the smallest concentration and the lowest with the highest concentration. Clear differences in the binding at the different pH values can be seen with the acidic compounds methotrexate and CDCF.

binding sites. Values for the parameters are presented in Tables 1 and 2, respectively. Figure 2 shows the measurements of timolol binding to melanin at pH 5.0 and their fit to the Sips (solid lines) and Langmuir (dashed lines) isotherms. For these data, both theoretical isotherms could be used, although the Scatchard plot suggests that the Sips isotherm is more adequate. The parameters of the Langmuir isotherm were obtained from the best fit in the direct plot, and the parameters of the Sips isotherm were obtained from the best fit in the log−log plot.

Methotrexate and CDCF binding at pH 7.4 was less than 4 and 8%, respectively, at all concentrations studied, and binding parameters were not calculated.

Figure 3 shows the measurements of chloroquine, methotrexate, nadolol, and CDCF binding to melanin at pH 5.0 and their fit to the Sips isotherm. The Scatchard plots (Figure 3b) are clearly nonlinear, and therefore, the Langmuir isotherm for one binding site class is not suitable to describe these data. The Sips isotherm incorporates the heterogeneity index n as a third fitting parameter, in addition to B_{max} and K_d, and is suitable to describe the binding data of these drugs because of two reasons. First, in the low concentration regime, the measurements lay on straight lines of slope $n < 1$ in a log−log plot. Second, the agreement between the experimental data and their Sips isotherm is excellent in the Scatchard plot, which is the more demanding of the two plots (a and b) considered in Figure 3.

The pH shift from pH 5.0 to pH 7.4 has a minor influence in the case of the basic compounds timolol and nadolol, and the binding data series for these pH values practically overlap in a log−log plot (Figure 4a). A similar conclusion is reached when overlapping (only pH 7.4 shown) the results for chloroquine at these pH values.

In addition to the Sips isotherm, the experimental binding data at both pH 5.0 and pH 7.4 were analyzed using the Langmuir isotherm for one and two classes of independent sites. The corresponding parameter values were obtained using two different methods, the best-fit in the direct plot (for two-site model see Table 2) and the best fit in the log−log plot. In all cases, the agreement between the experimental data and the fitted isotherms was worse than using the Sips isotherm (all data not shown).

Cell Studies. Cell uptake was studied with timolol, chloroquine, methotrexate, and CDCF in primary RPE cells. Timolol uptake ranged from 23−36% (Figure 5). Chloroquine uptake was much more substantial, about 99% with all the concentrations studied. Both methotrexate and CDCF uptake were so low that they were not detected based on the medium samples.

Drug elimination from the cells was studied with timolol and chloroquine during a 48 h time period. Timolol was completely eliminated from the cells within the 48 h experiment (Figure 6), and more than 85% was eliminated within the first 6 h. The elimination rate of chloroquine slowed down during the experiment, and over 88% of chloroquine was left inside in the end of the experiment.

Modeling. Uptake of timolol and chloroquine was simulated with 5−300 μg of melanin/well (75 000 cells). The amount of melanin had a significant effect on the amount of cell uptake according to the model as the fraction inside the cells increases with the increasing amount of melanin (Figure 7). In the case of chloroquine, the majority of the increase occurs within the range of 5−100 μg of melanin/well, but in the case of timolol, the increase continues throughout the whole range of 5−300 μg/well.

Radiolabeling of Chloroquine with ^{123}I. The main product of radiolabeling of chloroquine was 3-[I-123]-iodochloroquine. Radiochemical purity of the labeled product at the end of the synthesis was around 75%, and the specific activities were 464 MBq/mL and 153 MBq/mL for the study with the pigmented rats and with the albino rat, respectively. Radiolabeling yields were 30−45%. HPLC traces of radiolabeled chloroquine and elution conditions are shown in Figures S1 and S2 in the Supporting Information.

***In Vivo* Imaging.** Distribution of 3-[I-123]-iodochloroquine follows the same pattern in both the pigmented and albino rats except for the retention in the eyes of the pigmented rat. During the first 45 min, the drug or a radiometabolite is distributed into

Table 1. Binding Parameters Based on the Best Fit to the Sips Isotherm in the Log−Log Plot

Compound	n	B_{max} (nmol mg^{-1})	K_d (μM)	k^a
chloroquine pH 5	0.66 ± 0.05	80 ± 40	6 ± 7	23 ± 6
methotrexate pH 5	0.79 ± 0.01	164 ± 17	310 ± 60	1.74 ± 0.03
nadolol pH 5	0.95 ± 0.03	110 ± 70	500 ± 400	0.299 ± 0.016
CDCF pH 5	0.99 ± 0.03	19 ± 3	45 ± 12	0.436 ± 0.019
timolol pH 5	0.922 ± 0.025	84 ± 22	290 ± 120	0.457 ± 0.018
chloroquine pH 7.4	0.605 ± 0.012	380 ± 40	76 ± 23	27.9 ± 1.1
nadolol pH 7.4	0.94 ± 0.05	68 ± 24	340 ± 200	0.29 ± 0.03
timolol pH 7.4	0.95 ± 0.03	39 ± 6	120 ± 30	0.415 ± 0.016

$^a k \equiv B_{max}/K_d^n$. There are only three fitting parameters, n, B_{max}, and K_d.

DOI: 10.1021/acs.molpharmaceut.5b00787
Mol. Pharmaceutics 2016, 13, 2977−2986

Table 2. Parameter Values of the Isotherms of Two Classes of Independent Sites

Compound	B_{max1} (nmol mg^{-1})	K_{d1} (μM)	B_{max2} (nmol mg^{-1})	K_{d1} (μM)	k (nmol mg^{-1} μM^{-1})[a]
chloroquine pH 5	10.7 ± 0.6	0.093 ± 0.010	140 ± 30	37 ± 12	119 ± 7
methotrexate pH 5	39 ± 4	33 ± 5	1200 ± 220	(8 ± 17) × 10^3	1.33 ± 0.07
nadolol pH 5	0.22 ± 0.12	0.7 ± 1.1	108 ± 4	490 ± 30	0.5 ± 0.4
CDCF pH 5			19.3 ± 1.2	46 ± 7	0.42 ± 0.04
timolol pH 5	0.8 ± 0.6	2 ± 4	89 ± 5	310 ± 30	0.7 ± 0.6
chloroquine pH 7.4	43.3 ± 3	0.78 ± 0.15	268 ± 4	57 ± 3	59 ± 7
nadolol pH 7.4	2.1 ± 0.3	11 ± 3	79.7 ± 0.9	480 ± 15	0.355 ± 0.025
timolol pH 7.4	0.2 ± 0.3	1 ± 3	39.1 ± 0.8	120 ± 8	0.6 ± 1.0

[a] $k \equiv B_{max1}/K_{d1} + B_{max2}/K_{d2}$. There are four fitting parameters (e.g., B_{max1}, B_{max2}, K_{d1}, K_{d2}).

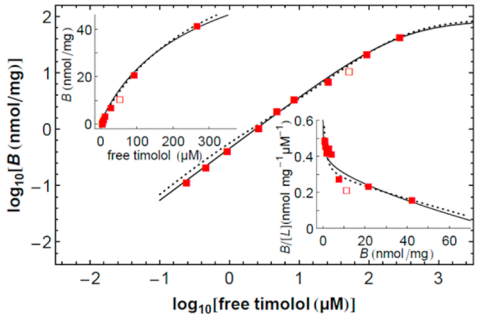

Figure 2. Timolol binding to melanin at pH 5.0 in log−log plot, direct (left insert), and Scatchard plots (right insert), the fit to the Sips isotherm with solid lines and Langmuir isotherm for two binding site classes with dotted lines. The open symbols mark a point that deviates significantly from the trend and has not been used in the fit; its inclusion would not lead to radically different results though.

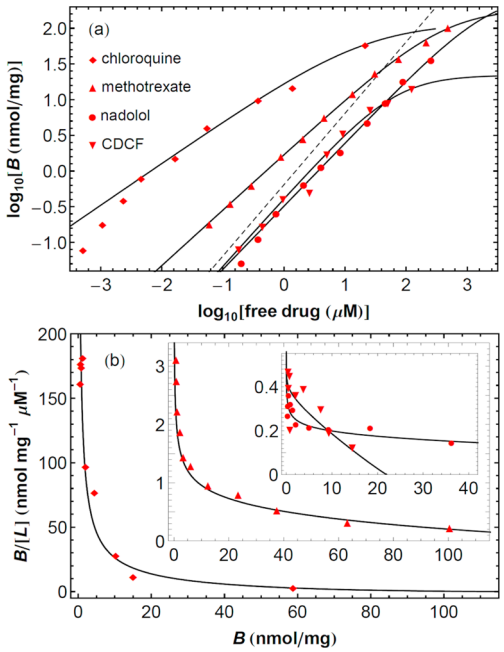

Figure 3. Experimental data of chloroquine, methotrexate, nadolol, and CDCF binding to melanin at pH 5.0 in a (a) log−log plot and (b) Scatchard plot, and their Sips isotherms (parameter values in Table 1). The dashed line in the log−log plot has a slope of one, and it has been introduced to highlight that the four isotherms have heterogeneity index $n < 1$, with n being the smallest for chloroquine and the largest for CDCF.

the liver, bladder, stomach, and the eyes (Figure 8). At 4 and 8 h, the activity continues to accumulate into the stomach but is also

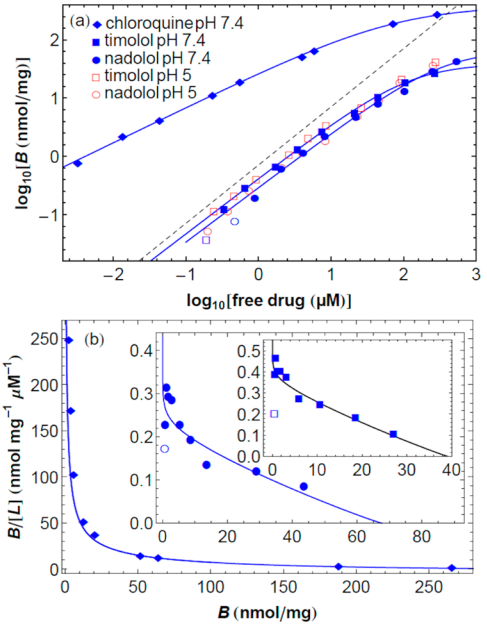

Figure 4. (a) Experimental data of chloroquine, timolol, and nadolol binding to melanin at pH 7.4. The dashed line has a slope of one, and it has been introduced to point out that the Sips isotherms (solid lines, parameter values in Table 1) have heterogeneity index $n < 1$. The binding measurements at pH 5.0 for timolol and nadolol have also been represented to highlight the minor influence of this pH shift for these drugs. (b) The Sips isotherms show an excellent agreement with the experimental data in the Scatchard plot. The point of lowest drug concentration in the pH 7.4 series of timolol and nadolol is an outlier and, hence, has not been used for the fit.

present in the bladder, the feces, and the eyes. At 24 h, activity is seen in the stomach of both rats. At this time, activity can also be seen in the thyroid of the albino rat. This is most likely caused by a radiometabolite, such as iodide. At 24 h, the drug or a radiometabolite is present in the eyes of the pigmented rats but not in the eyes of the albino rat.

A closer look to the head reveals the extent of 3-[I-123]-iodochloroquine accumulation into the eyes of the pigmented rat (Figure 9). Drug accumulation in the eyes becomes detectable during the first 15 min postinjection. The drug is located in the posterior part of the eyes and harderian glands. Small accumulation in the harderian glands is detected also in the albino rat until the time 8 h. At 24 h postinjection, 3-[I-123]-iodochloroquine is retained in ocular tissues of the pigmented rat, whereas in the albino rat, activity is only seen in the thyroid, most likely due to a radiometabolite such as iodide.

Activities in the ocular area were compared by quantitating the activity in the VOI drawn around the highest activity in the eyes,

DOI: 10.1021/acs.molpharmaceut.5b00787
Mol. Pharmaceutics 2016, 13, 2977−2986

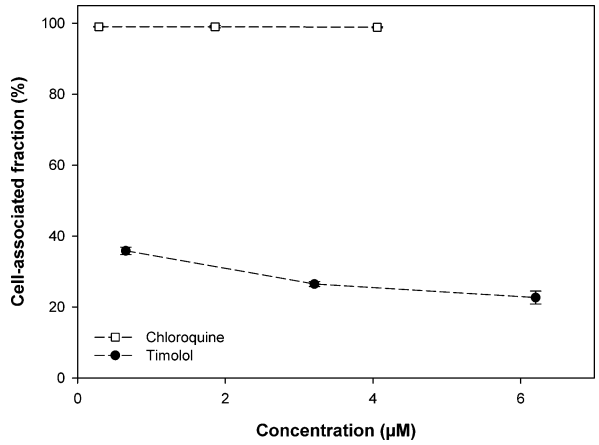

Figure 5. Uptake of timolol and chloroquine into pigmented RPE cells. Standard deviations are reported as error bars (generally covered by the symbol).

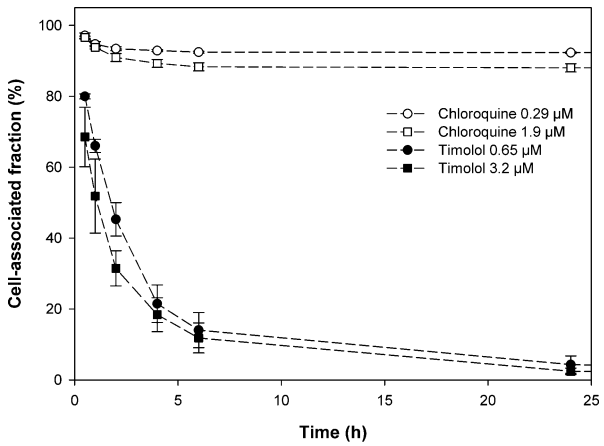

Figure 6. Elimination of timolol and chloroquine from primary RPE cells, on the *y*-axis the remaining cell-associated fraction as a percentage of the original cell-associated amount (at time 0 h). After 48 h, there was no timolol remaining associated with the cells, but based on calculations from samples taken from the medium above the cells, there was more than 88% of chloroquine remaining associated with the cells. Standard deviations are reported as error bars.

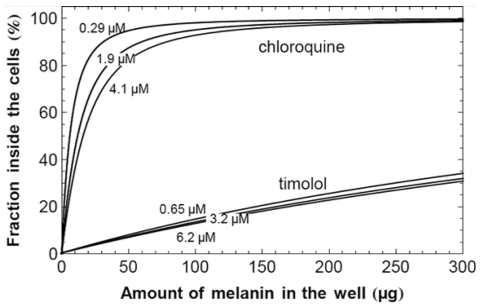

Figure 7. Modeling results for the effect of the amount of melanin inside the cells on the fraction of timolol and chloroquine inside the cells under equilibrium conditions, calculated for the concentrations used in the cell studies.

seen in Figure 9. Thus, in the pigmented rats, the VOIs of the time points 0−8 h represent the activity in the posterior part of the eyes and the harderian glands, and the last time point the activity only in the posterior part of the eyes. In the albino rat, VOIs were drawn at the harderian glands. The highest activity in the ocular area was achieved at 30 min after injection in one pigmented rat and 4 h after injection in the other pigmented rat and the albino rat (Figure 10). The activity is higher in the pigmented rats during the whole experiment.

DISCUSSION

There are multiple ways of calculating binding parameters of melanin binding studies.[8,10] The upward curvature of the binding curve in the Scatchard plot is often considered as an evidence for the existence of different classes of (independent) binding sites on the surface of the melanin granules. Despite its extended use in binding studies, the analysis based on the Scatchard plot has many critics, especially because of the different mechanisms that result in similar upward curvature.[12,13]

The hypothesis of several classes of independent sites is widely used because it is a simple model, it is integrated in most equipment software, and similar approaches are used frequently in pharmaceutical sciences (e.g., receptor, enzyme, and transporter studies). A relatively large number of fitting parameters leads to often good agreement between the fitted curve and the experimental data, but the reliability and physical meaning of the fitted values should be critically analyzed because the values are dependent on the drug concentrations that are used in the experiment. The upward curvature of the binding curve in the Scatchard plot is often considered as an evidence for the existence of multiple independent binding sites on the surface of the melanin granules, but this kind of curve might result from different mechanisms.[12,13] The Sips isotherm has proven to be a robust and physically meaningful approach to study binding of ions and drugs to melanin.[11,14] In this study, this approach was used successfully in the analysis of melanin binding data of timolol, chloroquine, nadolol, methotrexate, and CDCF.

The use of a robust Sips analysis and use of a broad concentration range in the experiments are essential in obtaining reliable estimates for the affinity and maximum binding capacity of melanin.[11] This would provide valuable background when melanin binding and its pharmacological consequences are estimated.

Ocular drug concentrations depend on the dosing, pharmacokinetics, and route of drug delivery. Drugs administered intravitreally reach much higher concentrations in ocular tissues than systemically administered drugs,[15] and the likelihood of accumulation into the pigmented tissues is greater. Strongly binding drugs, for example, chloroquine, can accumulate into pigmented ocular tissues even when given systemically, which shows that ocular pigment binding should be considered also in systemic therapy.[16,17] In line with *in vivo* profiles, chloroquine showed extensive melanin binding and retention in the pigmented cultured cells, whereas timolol was taken up into the pigmented cells, but it was retained in the cells only for a few hours. Timolol is known, however, to accumulate into pigmented ocular tissues of rabbits when given chronically as eye drops.[18,19] Evaluating the level of accumulation and time course of binding would require also studies on the dissociation rate of the drug from melanin.

Melanin binding studies were performed at pH 7.4 and 5.0. The lower pH represents the acidic environment of melanosomes where the binding to melanin takes place. Results of the acidic compounds CDCF (pK_a 5.1) and methotrexate (pK_a 4.1 and 3.4) were considerably different at the two pH values. As melanin is a polyanionic polymer, differences in binding of acidic compounds with pK_a close to 5.0 are expected since binding happens mainly through electrostatic interactions.[5,20] The

DOI: 10.1021/acs.molpharmaceut.5b00787
Mol. Pharmaceutics 2016, 13, 2977−2986

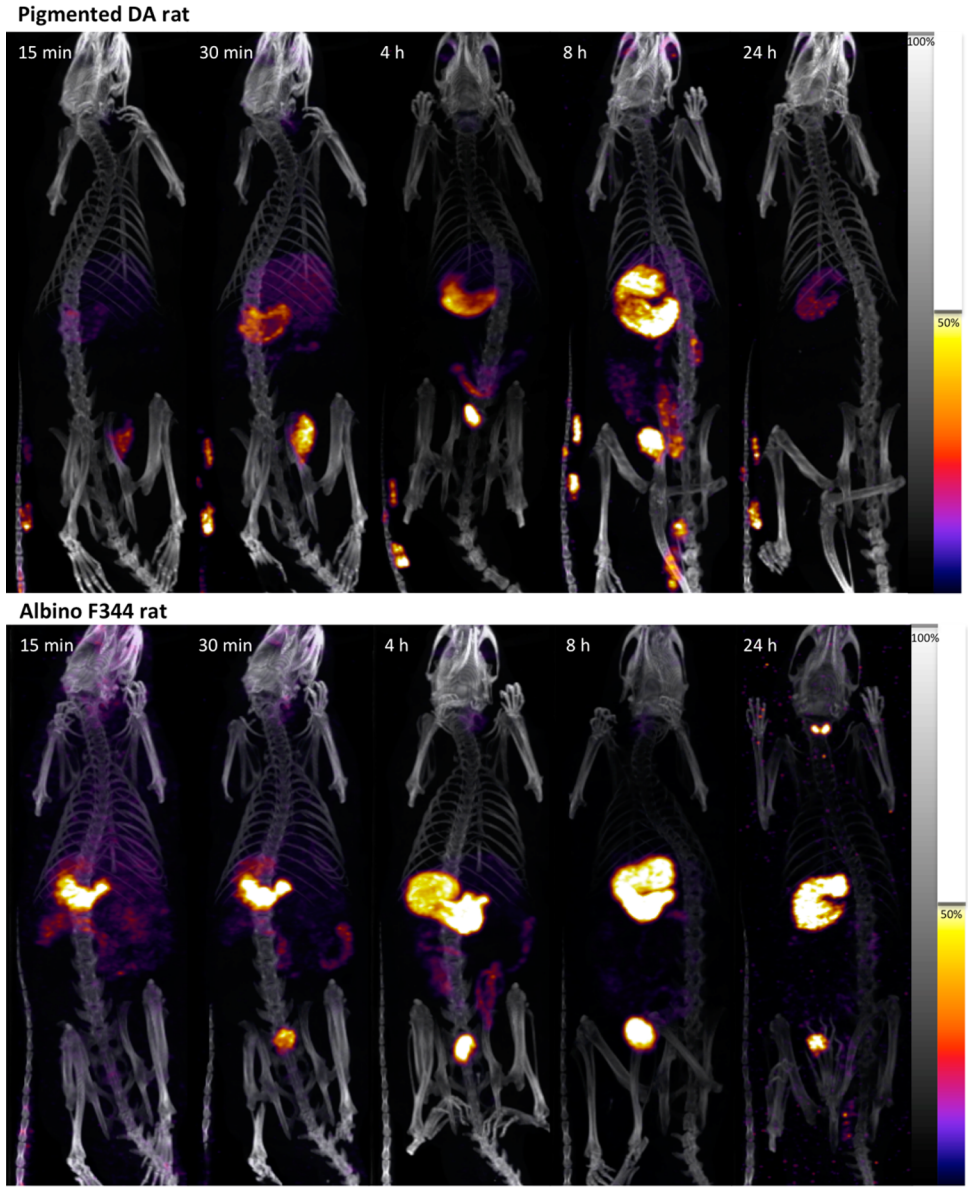

Figure 8. Distribution of 3-[I-123]-iodochloroquine in pigmented and albino rat. The scale represents the percentage of intensity used in the images. Distribution follows the same pattern in both rats except for the retention in the eyes of the pigmented rat.

change in pH also affects the ionization of melanin and thus affects the binding.[21] The change found here in the zeta potential of melanin granules is an indication of this. Bound percentages and affinity defined by the *k* value (Table 1) were similar to basic compounds chloroquine, timolol, and nadolol at both pH values. The compounds all have pK_a values above 8 (timolol and nadolol above 9); thus, the fraction ionized does not change considerably between the two pH values, and changes in binding are minor.

It is clear that melanin binding affects the amount of drug taken up by the primary RPE cells. The ratio between total compound concentration in the cells and compound concentration in the medium (K_p) is 140 for timolol and 25 200 for chloroquine at the smallest concentration studied. Comparing these to literature values of similar compounds obtained in cells without melanin shows that melanin binding largely effects cell uptake.[22] The K_p value of timolol obtained in this study is one order of magnitude higher and of chloroquine and two orders of magnitude higher than the ones obtained with similar compounds in melanin free cells.

To date, melanin binding has been included in pharmacokinetic models of ocular drug delivery only through permeability values of pigmented tissue layers.[23,24] There are many factors affecting permeability of cell membranes (incl. melanosome membrane) and cellular uptake that can affect drug exposure and binding to melanin. *In vitro* melanin binding studies do not take into account cell membrane permeability, expression of transporters, or pH changes inside cell compartments (cytoplasm, melanosomes) that can affect the access of the drug to melanin. In this study, a preliminary comparison of cell uptake results and predicted results based on *in vitro* binding parameters was done. Modeling results with parameters obtained at pH 7.4 correlated well with cell study results supporting the notion that effective melanin binding is a major governing factor in cellular drug distribution. However, at pH 5.0, the acidic compounds methotrexate and CDCF had considerable melanin binding, but they were not taken up into the pigmented cells, possibly due to their ionization and poor membrane permeability at pH 7.4.

DOI: 10.1021/acs.molpharmaceut.5b00787
Mol. Pharmaceutics 2016, 13, 2977−2986

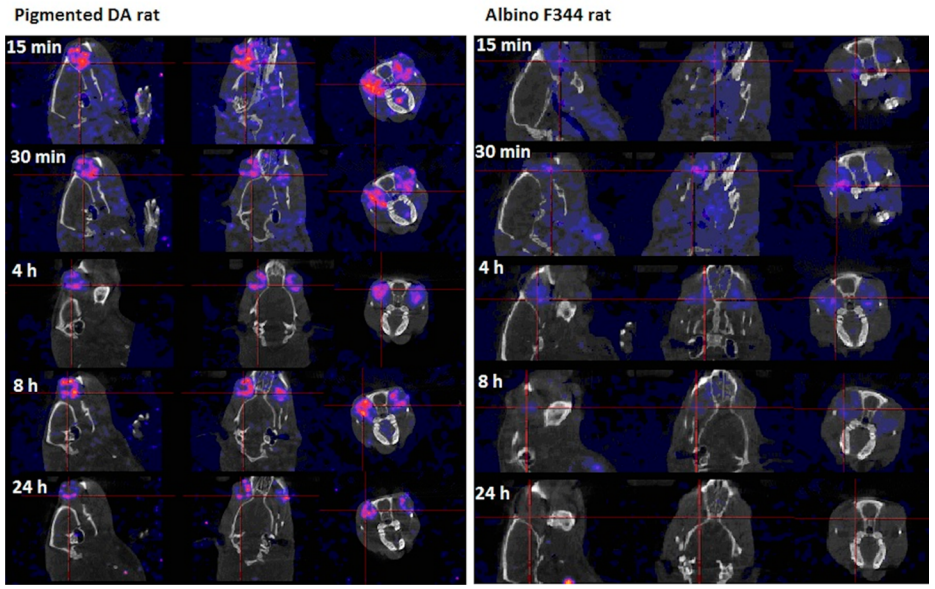

Figure 9. From left to right, sagittal, horizontal, and frontal slices of the head from pigmented rat and albino rat after 3-[I-123]-iodochloroquine administration. Already during the first 15 min, the drug or a radiometabolite is found in the eye of the pigmented rat. It is still retained there at the last time point. Drug accumulation in the harderian glands is seen in the albino rat until the time point 8 h. At the time point 24 h, there is no activity detected in the eyes of the albino rat.

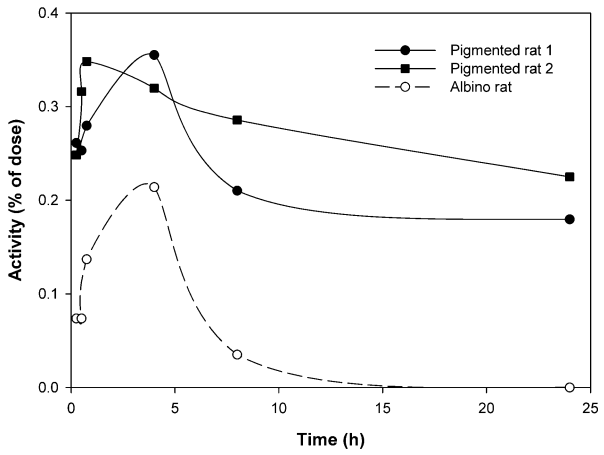

Figure 10. Activity of 3-[I-123]-iodochloroquine in the ocular area of the studied pigmented and albino rats normalized for the dose. Pigmented rat 1 corresponds to the pigmented rat in Figure 9. VOIs were drawn manually around the area of highest activity in the ocular area.

The amount of cellular melanin is a significant factor in the predictive potential of the model. In primary RPE cells, the amount of melanin may vary as a consequence of isolation method, duration of culture, and seeding density. According to Menon et al.,[25] there is 7.5 mg of melanin in human RPE-choroid. If the volume of RPE-choroid is assumed to be 10 μL[26] and the volume of the cells in the well 1 μL, the amount of melanin/well would be 750 μg. However, the amount is most likely smaller since melanin is not produced in primary RPE cells, and the melanin present at the isolation stage is divided among the cells as they divide. In this study, the amount was not determined, but different melanin amounts were simulated since there is no information about the amount of melanin in porcine RPE. The results showed that, in the case of timolol and chloroquine, cell uptake can be explained to a large extent by melanin binding, and at the levels of 200−300 μg of melanin/well, the melanin binding explains the entire extent of cell uptake. Melanin quantity in the RPE can vary with age,[27] and this might affect drug distribution to this tissue *in vivo* based on the relationship in Figure 7. Overall, this study shows the usefulness of melanin binding based prediction of cellular drug distribution.

This study demonstrates, for the first time, that melanin binding can be observed *in vivo* by SPECT/CT imaging. The results, although very preliminary (with two pigmented and one albino rat), show that *in vivo* kinetics regarding melanin binding can be studied with the method. The 3-[I-123]-iodochloroquine was seen accumulating to the ocular tissues of the pigmented rat but not the albino rat. Iodine radiotracers are a relevant choice of gamma radiators for melanin binding studies since they do not prevent melanin binding. However, it is important to note that the studied compound is not chloroquine but an iodinated analogue. Iodination may increase the octanol/water partitioning coefficient (log *P*) values and cause some increase in the melanin binding. The increase in lipophilicity may also change the access of drugs to pigmented tissues by increasing permeability through the blood−retinal barrier and lipid membranes. In summary, SPECT/CT imaging offers a noninvasive approach to study melanin-binding kinetics *in vivo* in rodents, but the radiotracer may modulate the binding to some extent.

■ CONCLUSIONS

We aimed to develop new methodological approaches to facilitate translation of melanin binding data to biological context. We showed that Sips algorithm was more suitable for the binding analysis of the five tested compounds. The binding parameters were successfully used to predict drug distribution to the RPE cells. Furthermore, SPECT/CT imaging was shown to be a useful tool to assess drug distribution to the pigmented tissues *in vivo*. In the future, these methods may help to predict and assess melanin binding of drugs in the pigmented tissues.

DOI: 10.1021/acs.molpharmaceut.5b00787
Mol. Pharmaceutics 2016, 13, 2977−2986

■ ASSOCIATED CONTENT

Supporting Information

The Supporting Information is available free of charge on the ACS Publications website at DOI: 10.1021/acs.molpharmaceut.5b00787.

HPLC traces of a typical chloroquine radiolabeling reaction; HPLC traces of radiolabeled chloroquine after cartridge purification (PDF)

■ AUTHOR INFORMATION

Corresponding Author

*E-mail: anna-kaisa.rimpela@helsinki.fi.

Notes

The authors declare no competing financial interest.

■ ACKNOWLEDGMENTS

This work was supported by the Academy of Finland (268868, 263573, 257786) (A.U., A.-K.R., and H.K.) and Sigrid Juselius foundation (64578) (A.U.). J.A.M. acknowledges the support from the Ministry of Economic Affairs and Competitiveness and FEDER (Project No. MAT2012-32084) and the Generalitat Valenciana (Project No. Prometeo/GV/2012/0069). We acknowledge Dr. Anu Airaksinen (University of Helsinki) for the kind advice and access to the radiochemistry laboratory. The UPLC analysis was kindly done by Timo Oksanen.

■ ABBREVIATIONS

CDCF, 5(6)-carboxy-2′,7′-dichlorofluorescein; DMEM, Dulbecco's modified Eagle medium; DMSO, dimethyl sulfoxide; DPBS, Dulbecco's phosphate buffered saline; EDTA, ethylenediaminetetraacetic acid; PBS, phosphate buffered saline; RPE, retinal pigment epithelium; SPECT/CT, single photon emission computed tomography/computed tomography; UPLC, ultraperformance liquid chromatography; VOI, volume of interest

■ REFERENCES

(1) Potts, A. M. The Reaction of Uveal Pigment in Vitro with Polycyclic Compounds. *Invest. Ophthalmol.* **1964**, *3*, 405−416.

(2) Hollo, G.; Whitson, J. T.; Faulkner, R.; McCue, B.; Curtis, M.; Wieland, H.; Chastain, J.; Sanders, M.; DeSantis, L.; Przydryga, J.; Dahlin, D. C. Concentrations of Betaxolol in Ocular Tissues of Patients with Glaucoma and Normal Monkeys after 1 Month of Topical Ocular Administration. *Invest. Ophthalmol. Visual Sci.* **2006**, *47* (1), 235.

(3) Salazar, M.; Shimada, K.; Patil, P. N. Iris Pigmentation and Atropine Mydriasis. *J. Pharmacol. Exp. Ther.* **1976**, *197* (1), 79−88.

(4) Potts, A. M. Toxic Responses of the Eye. In *Casarett and Doull's Toxicology. The Basic Science of Poisons*; Klaassen, C. D., Ed.; McGraw-Hill: New York, 1995; pp 583−615.

(5) Larsson, B.; Tjälve, H. Studies on the Mechanism of Drug-Binding to Melanin. *Biochem. Pharmacol.* **1979**, *28* (7), 1181−1187.

(6) Bhatnagar, V.; Anjaiah, S.; Puri, N.; Darshanam, B. N.; Ramaiah, A. pH of Melanosomes of B 16 Murine Melanoma Is Acidic: Its Physiological Importance in the Regulation of Melanin Biosynthesis. *Arch. Biochem. Biophys.* **1993**, *307* (1), 183−192.

(7) Fuller, B. B.; Spaulding, D. T.; Smith, D. R. Regulation of the Catalytic Activity of Preexisting Tyrosinase in Black and Caucasian Human Melanocyte Cell Cultures. *Exp. Cell Res.* **2001**, *262* (2), 197−208.

(8) Pitkänen, L.; Ranta, V.-P.; Moilanen, H.; Urtti, A. Binding of Betaxolol, Metoprolol and Oligonucleotides to Synthetic and Bovine Ocular Melanin, and Prediction of Drug Binding to Melanin in Human Choroid-Retinal Pigment Epithelium. *Pharm. Res.* **2007**, *24* (11), 2063−2070.

(9) Cheruvu, N. P. S.; Amrite, A. C.; Kompella, U. B. Effect of Eye Pigmentation on Transscleral Drug Delivery. *Invest. Ophthalmol. Visual Sci.* **2008**, *49* (1), 333−341.

(10) Pescina, S.; Santi, P.; Ferrari, G.; Padula, C.; Cavallini, P.; Govoni, P.; Nicoli, S. Ex Vivo Models to Evaluate the Role of Ocular Melanin in Trans-Scleral Drug Delivery. *Eur. J. Pharm. Sci.* **2012**, *46* (5), 475−483.

(11) Manzanares, J. A.; Rimpelä, A.-K.; Urtti, A. Interpretation of Ocular Melanin Drug Binding Assays. Alternatives to the Model of Multiple Classes of Independent Sites. *Mol. Pharmaceutics* **2016**, submitted.

(12) Gautam, L.; Scott, K. S.; Cole, M. D. Amphetamine Binding to Synthetic Melanin and Scatchard Analysis of Binding Data. *J. Anal. Toxicol.* **2005**, *29* (5), 339−344.

(13) Zierler, K. Misuse of Nonlinear Scatchard Plots. *Trends Biochem. Sci.* **1989**, *14* (8), 314−317.

(14) Bridelli, M. G.; Crippa, P. R. Theoretical Analysis of the Adsorption of Metal Ions to the Surface of Melanin Particles. *Adsorption* **2008**, *14* (1), 101−109.

(15) Del Amo, E. M.; Urtti, A. Current and Future Ophthalmic Drug Delivery Systems. A Shift to the Posterior Segment. *Drug Discovery Today* **2008**, *13* (3−4), 135−143.

(16) Tanaka, M.; Takashina, H.; Tsutsumi, S. Comparative Assessment of Ocular Tissue Distribution of Drug-Related Radioactivity after Chronic Oral Administration of 14C-Levofloxacin and 14C-Chloroquine in Pigmented Rats. *J. Pharm. Pharmacol.* **2004**, *56* (8), 977−983.

(17) Rosenthal, a R.; Kolb, H.; Bergsma, D.; Huxsoll, D.; Hopkins, J. L. Chloroquine Retinopathy in the Rhesus Monkey. *Invest. Ophthalmol. Vis. Sci.* **1978**, *17* (12), 1158−1175.

(18) Salminen, L.; Urtti, A. Disposition of Ophthalmic Timolol in Treated and Untreated Rabbit Eyes. A Multiple and Single Dose Study. *Exp. Eye Res.* **1984**, *38* (2), 203−206.

(19) Trope, G. E.; Menon, I. A.; Liu, G. S.; Thibodeau, J. R.; Becker, M. A.; Persad, S. D. Ocular Timolol Levels after Drug Withdrawal: An Experimental Model. *Can. J. Ophthalmol.* **1994**, *29* (5), 217−219.

(20) Ings, R. M. The Melanin Binding of Drugs and Its Implications. *Drug Metab. Rev.* **1984**, *15* (5−6), 1183−1212.

(21) Schroeder, R. L.; Pendleton, P.; Gerber, J. P. Physical Factors Affecting Chloroquine Binding to Melanin. *Colloids Surf., B* **2015**, *134*, 8−16.

(22) Mateus, A.; Matsson, P.; Artursson, P. Rapid Measurement of Intracellular Unbound Drug Concentrations. *Mol. Pharmaceutics* **2013**, *10*, 2467−2478.

(23) Ranta, V.-P.; Urtti, A. Transscleral Drug Delivery to the Posterior Eye: Prospects of Pharmacokinetic Modeling. *Adv. Drug Delivery Rev.* **2006**, *58* (11), 1164−1181.

(24) Amrite, A. C.; Edelhauser, H. F.; Kompella, U. B. Modeling of Corneal and Retinal Pharmacokinetics after Periocular Drug Administration. *Invest. Ophthalmol. Visual Sci.* **2008**, *49* (1), 320.

(25) Menon, I. A.; Wakeham, D. C.; Persad, S. D.; Avaria, M.; Trope, G. E.; Basu, P. K. Quantitative Determination of the Melanin Contents in Ocular Tissues from Human Blue and Brown Eyes. *J. Ocul. Pharmacol. Ther.* **1992**, *8* (1), 35−42.

(26) Ranta, V.-P.; Mannermaa, E.; Lummepuro, K.; Subrizi, A.; Laukkanen, A.; Antopolsky, M.; Murtomäki, L.; Hornof, M.; Urtti, A. Barrier Analysis of Periocular Drug Delivery to the Posterior Segment. *J. Controlled Release* **2010**, *148* (1), 42−48.

(27) Sarna, T.; Burke, J. M.; Korytowski, W.; Rózanowska, M.; Skumatz, C. M. B.; Zaręba, A.; Zaręba, M. Loss of Melanin from Human RPE with Aging: Possible Role of Melanin Photooxidation. *Exp. Eye Res.* **2003**, *76* (1), 89−98.

DOI: 10.1021/acs.molpharmaceut.5b00787
Mol. Pharmaceutics 2016, 13, 2977−2986

Supporting Information

Drug distribution to retinal pigment epithelium: studies on melanin binding, cellular kinetics, and single photon emission computed tomography/computed tomography imaging

Anna-Kaisa Rimpelä[a], Mechthild Schmitt[a], Satu Latonen[a], Marja Hagström[a], Maxim Antopolsky[a], José A. Manzanares[c], Heidi Kidron[a], Arto Urtti[a,b]

[a] Centre for Drug Research, Division of Pharmaceutical Biosciences, Faculty of Pharmacy, University of Helsinki, P.O. Box 56, FI-00014 University of Helsinki, Finland

[b] School of Pharmacy, University of Eastern Finland, P.O. Box 1627, FI-70211 Kuopio, Finland

[c] Department of Thermodynamics, Faculty of Physics, University of Valencia, E-46100 Burjassot, Spain

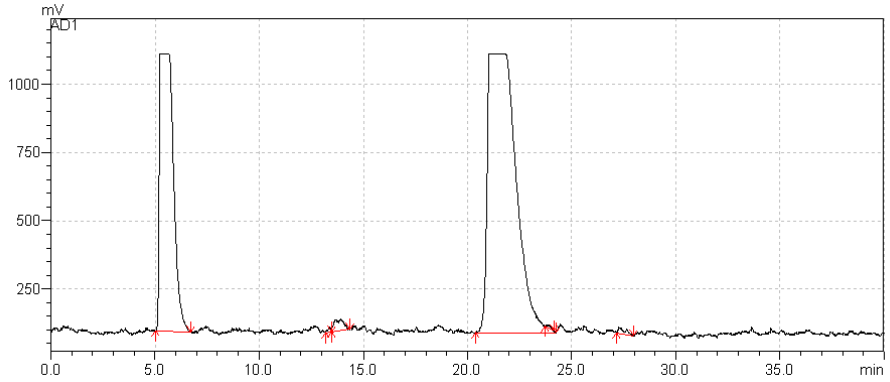

Figure S1. HPLC traces of a typical chloroquine radiolabeling reaction. A - 0.05 M NaH_2PO_4 buffer, B – 0.05 M NaH_2PO_4 buffer in 70 % MeCN, pH = 5.0. Linear gradient from 0 to 70 % B in 30 min. Peak at 22 min corresponds to the target compound; peak at 6 min corresponds to unreacted ^{123}I.

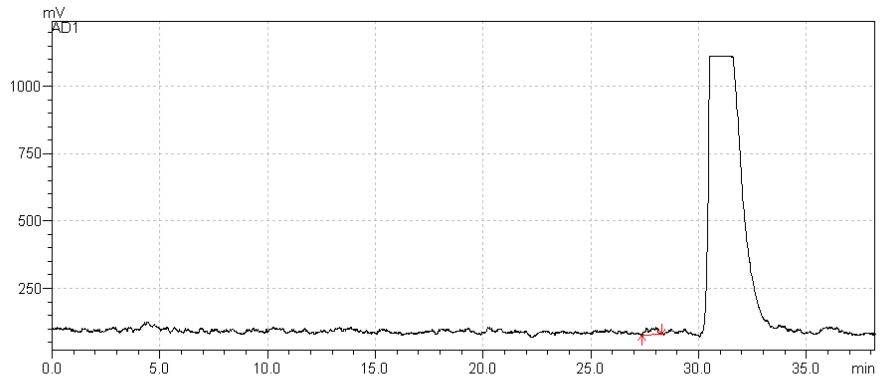

Figure S2. HPLC traces of radiolabeled chloroquine after cartridge purification. A - 0.05 M NaH_2PO_4 buffer, B – 0.05 M NaH_2PO_4 buffer in 70% MeCN, pH = 5.0. Linear gradient from 0 to 50 % B in 30 min. Peak at 32 min corresponds to the target compound.